The Stress Variations in a Mating Plastic Spur Gear Pair

Ah-Der Lin[1], Jao-Hwa Kuang[2]

[1]Dept. of Mech. Eng., Cheng Shiu University, Kaohsiung 80833, Taiwan

[2] Dept. of Mech. and Electro-Mech. Engineering, National Sun Yat-Sen University, Kaohsiun, 80424, Taiwan

kuang@faculty.nsysu.edu.tw

Abstract - A dynamic model of an engaging spur gear pair is proposed to study the distributions and variation of bending and surface contact stresses around the fillet and contacting points for plastic gears. The parameters used in this dynamic model include time-varying mesh stiffness, frictional coefficient, and profile-shifted factor, etc. Due to high sensitivity to heat for plastic material, the influence of temperature on plastic gears has also been taken into consideration in this work. A computational algorithm is developed to simulate the variation of fillet bending and surface contact stresses during the engagement with different speeds. The results indicate that the operating temperature may affect the distribution and the magnitude of bending and surface contact stresses of a plastic gear pair significantly.

Keywords -Stress. Plastic gear pair.

I. INTRODUCTION

For metallic gears, the bending and surface stresses have been widely discussed. Considering the tooth surface contact stress, operating temperature, and film of lubrication, Seireg and Conry [1] proposed a lumped parameter to indicate the optimal tooth surface durability. In 1970, Gay [2] discussed the sliding wear of an engaging gear pair. To obtain a lumped parameter about the tooth surface wear and pitting, the velocities were investigated at initial contact point (IP), lowest point of single tooth contact point (LPSTC), pitch point (PP), highest point of single tooth contact (HPSTC), and final contact point (FP) along the path of contact. The fatigue-life model of rolling-element bearing was applied to gear elements by Coy, Townsend, and Zaretsky [3]. Using the constant of proportionality related to material, the surface fatigue life was built, and the results of experiment were shown to prove the validity of the proposed model. Moore [4] discussed the bending and tooth surface fatigues at very-high-load cycles, and the subsequent effect was also included in his study. Given gear ratio, pinion torque and allowable stress of a standard spur gear pair, the optimal gear size was analyzed by Savage, Coy and Townsend [5]. In the study, pitting fatigue, bending fatigue, interference and gear ratio were investigated under the situation of static load. Then, Carroll and Johnson [6] expanded the results by Savage, Coy and Townsend to obtain a optimal design method for an gear pair. In the model, geometric and dynamic factors of AGMA standard were included. In 1985, Lin and Sereg [7] provided a computer-based procedure for the optimization of a gear train. A lumped parameter, consisting of strength, surface durability, wear resistance and tooth surface temperature, was proposed to improve the load-carrying capacity of an engaging gear pair. Carroll and Johnson [8] presented a non-dimensional factor, the material properties relationship factor, to discuss undercut, bending stress and surface contact stress. In 1991, Errichello [9] used a static load model to analyze undercut, bending fatigue, surface fatigue and tooth surface sliding wear. Mobie [10, 11] published several papers about equal strength design. In his analysis, the parameters, such as profile-shifted factor, mesh stiffness, were considered. As to the dynamic effects of an engaging gear pair, many tooth pair dynamic models have been introduced. A number of numerical methods, e.g., the methods proposed by Wang [12], Yang [13], Arikan [14] and Kuang [15], have been employed to calculate the dynamic contact load or the torsional response. The effects of nonlinear parameters, i.e., tooth errors, addendum modification, mesh stiffness, damping factor and friction coefficient, on the dynamic loads have also been widely discussed [16].

For plastic gears, however, the strength is still under investigation. Due to the high sensitivity of plastic material to temperature, the parameters of a plastic gear pair are more complicated than those of a metallic gear pair. Tsukamoto [17] has studied the life of an engaging plastic gear pair from 1984. In his studies, the experimental results were presented and used to describe the life of plastic gears. In 1986, Tsukamoto [18] also proposed a method to extend the life of an engaging plastic gear pair. Different materials of a plastic gear pair were discussed, such as Nylon-steel, Nylon-nylon, and POM-POM [19, 20] gear pair.

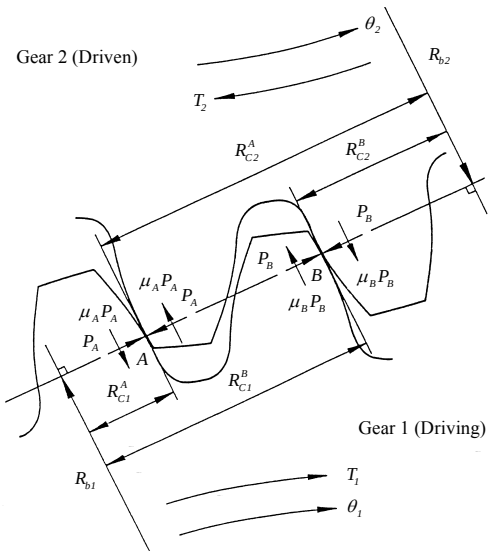

Figure 1: The free body diagram of a spur gear pair.

II. DYNAMIC MODEL FOR A SPUR GEAR PAIR

An engaged spur gear pair is shown in Fig. 1, in which T_1 and T_2 denote the input and output torque respectively. The radii of the base circles of the engaged gear pair are R_{b1} and R_{b2}, respectively. The dynamic contact loads at the contact points A and B are P_A and P_B. The radii of curvatures at the mating points are R_{c1}^i and R_{c2}^i ($i = A,B$) for gears *1* and *2*, respectively. The instantaneous coefficients of friction at the contact points are μ_A and μ_B. The angular displacements of gear *1* and gear *2* are denoted by θ_1 and θ_2. The equations of motion for gears *1* and *2* can be written as

$$J_1\ddot{\theta}_1 = T_1 - R_{b_1}(P_A + P_B) \pm R_{c_1}^A \mu_A P_A \mp R_{c_1}^B \mu_B P_B \quad (1)$$

$$J_2\ddot{\theta}_2 = R_{b_2}(P_A + P_B) - T_2 \mp R_{c_2}^A \mu_A P_A \pm R_{c_2}^B \mu_B P_B \quad (2)$$

where J_1 and J_2 are the polar moments of inertia of gears *1* and *2*, respectively. Along the line of action, the displacements of gears *1, 2* are

$$\delta_1 = R_{b1}\theta_1 \quad (3)$$

$$\delta_2 = R_{b2}\theta_2 \quad (4)$$

Therefore, the relative displacement between the two gears can be written as:

$$\delta_r = R_{b_1}\theta_1 - R_{b_2}\theta_2 \quad (5)$$

The effective masses of the two engaging gears are

$$M_1 = J_1 / R_{b1}^2 \quad (6)$$

$$M_2 = J_2 / R_{b2}^2 \quad (7)$$

Consider that ε_A and ε_B are the composite profile deviations at the mating points *A* and *B*. The dynamic loads at contact points *A* and *B* can be calculated using the following:

$$P_A = K_A(\delta_r - \varepsilon_A) \quad (8)$$

$$P_B = K_B(\delta_r - \varepsilon_B) \quad (9)$$

It is assumed that the dynamic alternation of output torque T_2 is so small that

$$T_1 / R_{b1} \approx T_2 / R_{b2} \quad (10)$$

The converted equation of motion with relative displacement δ_r can be derived as

$$\ddot{\delta}_r + \omega_n^2 \delta_r = \xi_r \quad (11)$$

With

$$\omega_n^2 = \frac{1}{M_1 M_2}[K_A(G_1^A M_2 + G_2^A M_1) + K_B(G_1^B M_2 + G_2^B M_1)]$$

$$\xi_r = \frac{1}{M_1 M_2}[(M_1 + M_2)P_0 + K_A\varepsilon_A(G_1^A M_2 + G_2^A M_1) + K_B\varepsilon_B(G_1^B M_2 + G_2^B M_1)]$$

$G_1^A = 1 \mp R_{c_1}^A \mu_A / R_{b_1}$, (- for approach; + for recess)

$G_1^B = 1 \pm R_{c_1}^B \mu_B / R_{b_1}$, (+ for approach; - for recess)

$G_2^A = 1 \mp R_{c_2}^A \mu_A / R_{b_2}$, (- for approach; + for recess)

$G_2^B = 1 \pm R_{c_2}^B \mu_B / R_{b_2}$, (+ for approach; - for recess)

where P_0 is the reference load or the steady load, $P_0 = T_1 / R_{b_1}$. The effect of the damping force is incorporated into the dynamic load calculation by introducing a viscous damping force $2\zeta\omega_n\dot{\delta}_r$. Under this assumption, the converted equation of motion can be rewritten as:

$$\ddot{\delta}_r + 2\zeta\omega_n\dot{\delta}_r + \omega_n^2\delta_r = \xi_r \quad (12)$$

Based on the experimental results [21], the magnitude of damping ratio ζ is assumed to be *0.6* in this study.

III. PARAMETERS FOR THE DYNAMIC EQUATION

A. Position dependent mesh stiffness

The mesh stiffness between an engaged gear pair consists of two parts; one associated with the local Hertzian deformation and the other associated with the tooth bending deflection. The unit width Hertzian stiffness $\bar{K}_h$ resulting from the tooth surface contact was first approximated by Yang [13] as:

$$\bar{K}_h = \pi E / \left[4(1-\nu^2)\right] \quad (13)$$

where E is Young's module and ν is the Poisson's ratio. It was noticed that the unit width Hertzian stiffness is related only to the gear material, and remains constant along the path of contact.

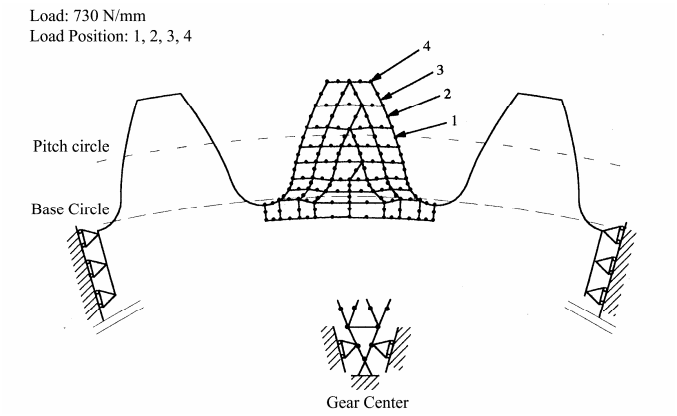

Figure 2: The finite element model of a plastic gear.

Figure 2 is the corresponding finite element model of a standard involute spur gear. The gear material is Nylon 66 and the ambient temperature is 20^0C. With the finite element results, an equation for the tooth bending stiffness is curve fitted. The unit width stiffness $\bar{K}_{Nylon}^*$ for a single tooth *i* at a loading position *r* can be approximated by the following equation.

$$\bar{K}_{Nylon}^* = (A_0 + A_i X_i) + (A_2 + A_3 X_i)\frac{(r - R_i)}{(1 + X_i)\cdot m} \quad (14)$$

where X_i and N_i denote the profile shifting coefficient and the number of teeth of gear *i*. The loading position *r* is a radial distance originated from the gear center. The radius of pitch circle R_i and the module *m* in the Eq. (14) are

measured in the same unit (mm). The curve fitted coefficients for a Nylon gear are

$$A_0 = 307.2 + 1.262N_i + 2.325\times10^{-5}N_i^2 - 5.840\times10^{-5}N_i^3$$
$$A_1 = 461.4 - 5.778N_i + 8.035\times10^{-2}N_i^2 - 3.591\times10^{-4}N_i^3$$
$$A_2 = -240.5 + 1.269N_i - 3.582\times10^{-5}N_i^2 + 2.279\times10^{-4}N_i^3$$
$$A_3 = -380.7 + 3.796N_i - 6.705\times10^{-5}N_i^2 + 3.858\times10^{-4}N_i^3$$

At the same temperature, the single tooth stiffness per unit width of a plastic gear depends on the Young's modulus of the gear material. For plastic gears at the ambient temperature 20^0C, it is assumed that a linear relationship is existed between the bending stiffness and Young's modulus. Taking the POM gear for example, the following equation might be used to approximate the bending stiffness.

$$\bar{K}^*_{POM} = \bar{K}^*_{Nylon}\cdot\frac{E^*_{POM}}{E^*_{Nylon}} \quad (15)$$

where E^*_{Nylon} and E^*_{POM} are the Young's moduli of Nylon and POM at 20^0C respectively. The ratio of E^*_{POM} to E^*_{Nylon} is a value between *1.4* and *1.6*. It is assumed to be *1.5* in this paper. It is noted that the stiffness of a plastic gear is affected significantly by temperature. The stiffness of a Nylon gear at different temperature $T\ (^\circ K)$ can be curve fitted as [19]

$$\bar{K}_{Nylon}(T) = \bar{K}^*_{Nylon}\cdot f_{Nylon}(T) \quad (16)$$

where

$$f_{Nylon}(T) = E_{Nylon}(T)/E^*_{Nylon} = -1.929\cdot\ln(T) + 11.949$$

Similarly, the equation for a POM gear can be written as [22]

$$\bar{K}_{POM}(T) = \bar{K}^*_{Nylon}\cdot f_{POM}(T) \quad (17)$$

where

$$f_{POM}(T) = E_{POM}(T)/E^*_{Nylon} = -1.775\cdot\ln(T) + 11.574 \quad (18)$$

The single tooth pair stiffness K_A and K_B at contact points *A* and *B* can be approximated by combining the unit width stiffness $\bar{K}_1(r_{1A})$, $\bar{K}_2(r_{2A})$, $\bar{K}_1(r_{1B})$, $\bar{K}_2(r_{2B})$ and $\bar{K}_h$ of mating teeth as springs connected in series. It should be noted that the values of $\bar{K}_1(r_{1A})$, $\bar{K}_2(r_{2A})$, $\bar{K}_1(r_{1B})$, $\bar{K}_2(r_{2B})$ depend on the gear material, the ambient temperature and the loading position.

$$\frac{K_A}{F} = \frac{\bar{K}_1(r_{1A})\bar{K}_2(r_{2A})\bar{K}_h}{\bar{K}_1(r_{1A})\bar{K}_2(r_{2A}) + \bar{K}_1(r_{1A})\bar{K}_h + \bar{K}_2(r_{2A})\bar{K}_h} \quad (19)$$

$$\frac{K_B}{F} = \frac{\bar{K}_1(r_{1B})\bar{K}_2(r_{2B})\bar{K}_h}{\bar{K}_1(r_{1B})\bar{K}_2(r_{2B}) + \bar{K}_1(r_{1B})\bar{K}_h + \bar{K}_2(r_{2B})\bar{K}_h} \quad (20)$$

where K_A and K_B represent the single tooth pair stiffness of gears *1, 2* at contact points *A* and *B*.

B. Temperature rise effect

According to the experimental results by Tsukamoto [19, 23], the temperature rise of a running plastic gear pair is related to the product of P and V. In Tsukamoto's model [23], P is the equivalent Hertzian stress calculated by assuming the engaged gear pair as steel gears, and V is the mean sliding speed on the tooth profile. They lead to

$$P = \left\{\frac{4T_1}{\pi F}\frac{E'(N_1+N_2)}{N_1^2N_2m^2\sin\phi\cos\phi}\right\}^{1/2} \quad (21)$$

$$V = \left\{C_x\sin\phi_x - \frac{(N_1+N_2)}{N_2}\cdot\sqrt{R_{O2}^2 - R_{b2}^2}\right\}\cdot\pi n_1 \quad (22)$$

where

$R_{O2} = N_2m/2 + Xm + m$

$R_{b2} = (N_2m/2)\cdot\cos\phi$

C_x : the center distance

n_1 : the operating speed of gear *1*

ϕ : the pressure angle of the standard involute tooth

ϕ_x : the operating pressure angle of profile-shifted gear pair

E' : the effective Young's modulus

The effective Young's modulus is defined as

$$\frac{1}{E'} = \frac{1-\nu_1^2}{E_1} + \frac{1-\nu_2^2}{E_2} \quad (23)$$

where $E_1 = E_2 = 207\,(\text{GPa})$ and $\nu_1 = \nu_2 = 0.3$.

Based on experimental results [23], the temperature rise of an engaged plastic gear pair can be estimated by

POM-POM : $\Delta T = 0.07150\cdot(PV) - 0.5139$ (24)

Nylon-Nylon : $\Delta T = 0.06802\cdot(PV) - 0.5232$ (25)

where the units of ΔT 、P、V are °K 、MPa and m/s respectively.

C. Frictional coefficients

According the reference paper [24], the friction coefficient may be approximated as *0.2* and *0.3* for the Nylon-Nylon and the POM-POM gear pairs respectively.

D. Polar mass moment of inertia

The polar moment of inertia of a solid addendum modified involute spur gear *i* can be approximated by a curve fitted equation.

$$J_i = \left(\frac{\pi N_i}{32} + B_0X_i\right)m^4\rho F \quad (26)$$

where N_i, F and ρ are the tooth number, tooth face width and density of the gear *I*, respectively. The coefficient in equation [25] is

$$B_0 = -2.8182 + 2.6774N_i - 8.3738N_i^2 + 0.8443N_i^3$$

The m odule m and the face width F in Eq. (27) are all measured in m eters. The density ρ and the inertia J are measured in ($\mathrm{kg/m^3}$) and ($\mathrm{kg \cdot m^2}$).

E. Bending stress

According Kuang and Yang [25], the bending stress at the contact points can be express as

$$\sigma_b = K_f \sigma_{ref} \quad (27)$$

where K_f and σ_b are the stress intensity factor and reference bending stress respectively.

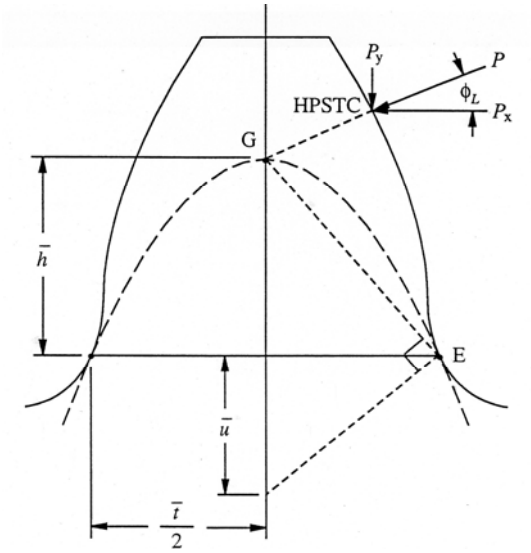

Figure 3: The dynamic contact load at HPSTC.

Using finite method and curve fitting methods, as shown in Fig. 3, the reference bending stress is defined at the highest point of single tooth contact point (HPSTC), and can be written as

$$\sigma_{ref} = \frac{6P\bar{h}\cos\phi_L}{\bar{t}^2} - \frac{P\sin\phi_L}{\bar{t}} \quad (28)$$

The stress intensity factor can be expressed as

$$K_f = \sum_{j=1}^{4} K_{fj} \left[\prod_{\substack{i=1 \\ i\neq j}}^{4} \frac{r - r_i}{r_j - r_i} \right] \quad (29)$$

where

$$r_i = \frac{(i-1)(1+X)m}{3} + \frac{Nm}{2} \quad (i = 1 \sim 4)$$

$$K_{fj} = \xi_j + \eta_j \left[\ln(N)\right] + \zeta_j \left[\ln(N)\right]^2 \quad (j = 1,2,3,4)$$

$$\xi_1 = 3.04824 - 5.95778X - 48.3892X^2 - 3.48589X^3 + 126.074X^4$$
$$\xi_2 = 3.40968 + 0.63141X - 31.9999X^2 - 7.48930X^3 + 102.017X^4$$
$$\xi_3 = 2.58298 - 0.35845X - 13.2569X^2 - 7.24413X^3 + 46.5878X^4$$
$$\xi_4 = 2.58406 - 1.21402X - 6.74703X^2 - 2.40483X^3 + 25.6754X^4$$
$$\eta_1 = -0.69543 + 4.68270X + 27.8550X^2 - 4.43505X^3 - 77.1001X^4$$
$$\eta_2 = -0.93543 + 0.38605X + 17.4744X^2 + 3.40209X^3 - 53.4126X^4$$
$$\eta_3 = -0.58586 + 0.71657X + 7.31048X^2 + 3.11869X^3 - 24.1617X^4$$
$$\eta_4 = -0.62757 + 0.93156X + 3.64696X^2 + 0.70227X^3 - 13.3626X^4$$
$$\zeta_1 = 0.14383 - 0.70639X - 3.83054X^2 + 2.59095X^3 + 13.1661X^4$$
$$\zeta_2 = 0.14413 - 0.06252X - 2.26575X^2 - 0.35485X^3 + 6.85501X^4$$
$$\zeta_3 = 0.09498 - 0.11956X - 0.98598X^2 - 0.33977X^3 + 3.10444X^4$$
$$\zeta_4 = 0.09498 - 0.13658X - 0.47936X^2 - 0.03947X^3 + 1.70043X^4$$

According to the references [26, 27], the strength of Nylon and POM can be curve-fitted and expressed as

$$\sigma_b^*(T)_{Nylon} = 1512\exp\left(-9.985\times10^{-3}T\right) \quad (30)$$

$$\sigma_b^*(T)_{POM} = -0.705T + 298.965 \quad (31)$$

where the units for σ_b^* and T are MPa and ^{0}K respectively. Let the safety factor for bending stress be $\sigma_b^* / (\sigma_b)_{\max}$, where $(\sigma_b)_{\max}$ is the m aximum bending stress at the temperature described by σ_b^*.

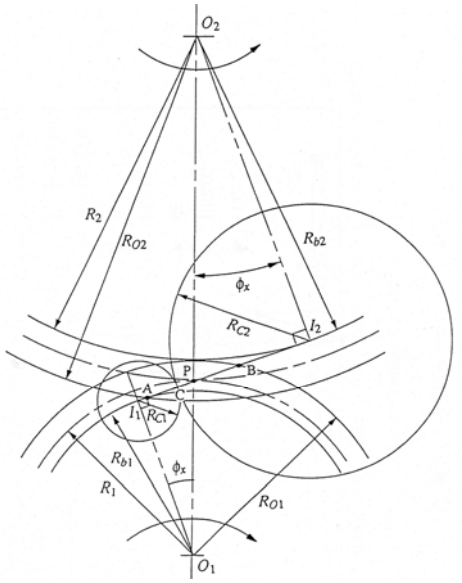

Figure 4: Curvature at the contact point.

F. Surface contact stress

As shown in Fig. 4 the analytic model for surface contact stress proposed by Smith [28] is used. Let x, y, and z be the tangential, axial and radial directions at the contact point. Assuming the plane strain case at the contact point, the stresses at xz plane can be written as

$$\sigma_x = -\frac{p_0}{\pi}\left\{\left(a_0^2 + 2x^2 + 2z^2\right)\frac{z}{a_0}\bar{\varphi} - 2\pi\frac{z}{a_0}3xz\varphi\right.$$
$$\left.\mu\left[\left(2x^2 - 2a_0^2 - 3z^2\right)\varphi + 2\pi\frac{x}{a_0} + 2\left(a_0^2 - x^2 - z^2\right)\frac{x}{a_0}\bar{\varphi}\right]\right\} \quad (32)$$

$$\sigma_y = -\frac{2\nu}{\pi}p_0\left\{\left[\left(a_0^2 + x^2 + z^2\right)\frac{z}{a_0}\bar{\varphi} - \frac{\pi z}{a_0} - 2xz\varphi\right]\right.$$
$$\left.+\mu\left[\left(x^2 - a_0^2 - z^2\right)\varphi + \frac{\pi x}{a_0} + \left(a_0^2 - x^2 - z^2\right)\frac{x}{a_0}\bar{\varphi}\right]\right\} \quad (33)$$

$$\sigma_z = -\frac{p_0}{\pi} z\left(a_0\bar{\varphi} + x\varphi + \mu z\varphi\right) \quad (34)$$

$$\tau_{xz} = -\frac{p_0}{\pi}\left\{z^2\varphi + \mu\left[\left(a_0^2 + 2x^2 + 2z^2\right)\frac{z}{a_0}\bar{\varphi}\right] - 2\pi\frac{z}{a_0} - 3xz\varphi\right\} \quad (35)$$

where p_0 the maximum surface pressure, μ is the frictional coefficient. The semi Hertzian contact width at point *A*, a_0, is determined using

$$a_o = 4\left(P_A R_A / 2\pi E' F\right)^{1/2} \quad (36)$$

As shown in Fig. 4, the equivalent radius R_A at the contact point *A* is dependent upon the radii of curvature of gears 1 and 2, which is defined as

$$R_A = R_{C1}^A R_{C2}^A / (R_{C1}^A + R_{C2}^A) \quad (37)$$

φ and $\bar{\varphi}$ can be written as

$$\varphi = \frac{\pi}{\lambda_1}\frac{1-\lambda_3}{\lambda_3\sqrt{2\lambda_3+\lambda_4}} \quad (38)$$

$$\bar{\varphi} = \frac{\pi}{\lambda_1}\frac{1+\lambda_3}{\lambda_3\sqrt{2\lambda_3+\lambda_4}} \quad (39)$$

where $\lambda_1 = \left(a_0 + x\right)^2 + z^2$, $\lambda_2 = \left(a_0 - x\right)^2 + z^2$, $\lambda_3 = \left(\lambda_2/\lambda_1\right)^{1/2}$ and $\lambda_4 = \left(\lambda_1 + \lambda_2 - 4a_0^2\right)/\lambda_1$.

Using eqns (33)~ (36), the pri nicipal stresses and the maximum shear stress at $z = 0$ can be calculated. For Nylon, the compressive strength σ_h^* can be express in terms of temperature as [26]

$$\sigma_h^*(T)_{Nylon} = -0.82T + 345.593 \quad (40)$$

where the units for σ_h^* and T are MPa and ^{0}K respectively. Let the safety factor for suface contace stress be $\sigma_h^*/(\sigma_h)_{\max}$, where $(\sigma_h)_{\max}$ is the m aximum bending stress at the temperature desribed by σ_h^*.

IV. DYNAMIC LOAD AND STRESS SIMULATION

A quasi-linear iteration procedure modified from the method proposed by Arikan *et al.* [19] was used to calculate the dynamic loads. The basic assumptions for this simulation include the following:

1. Gears *1* and *2* are loaded respectively with constant torques T_1 and T_2. Both are proportional in magnitude but opposite in sign.
2. The line of action remains fixed during gear meshing.
3. Four mesh points are used to represent the successive positions of an engaging toot h-pair in loading. They are the initial contact point of engagem ent, *IP,* the lowest point of single-tooth contact, *LPSTC*; the highest point of single-tooth contact, *HPSTC*; and the final contact point of engagem ent, *FP*. The relative displacement δ_r and the instantaneous velocity $\dot{\delta}_r$ at the cyclic contacting points must be equal; i.e. $(\delta_r)_{IP} = (\delta_r)_{HPSTC}$, $(\delta_r)_{LPSTC} = (\delta_r)_{FP}$, and $(\dot{\delta}_r)_{IP} = (\dot{\delta}_r)_{HPSTC}$, $(\dot{\delta}_r)_{LPSTC} = (\dot{\delta}_r)_{FP}$

The time interval from the initial contact point, *IP,* to the highest point of si ngle tooth contact, *HPSTC,* is considered as one loading period τ. In this quasi-linear iteration method, the period is divided into m any small intervals $\Delta\tau$. Within an interval, the position dependent parameters ω_n and ξ_r of the equation of m otion are considered as constants and the analytical solution is obtained. Starting with the initial estim ates of $\delta_r(0)$ and $\dot{\delta}_r(0)$ at the initial contact point, the values δ_r and $\dot{\delta}_r$ are calculated at the end of each interval by taking the values of δ_r and $\dot{\delta}_r$ at the end of the previous interval as the initial conditions for the next time interval. If the calculated values of $\delta_r(\tau)$, $\dot{\delta}_r(\tau)$ differ from the guessed $\delta_r(0)$ $\dot{\delta}_r(0)$, an iteration procedure is used to obtain the *(i+1)*th iteration values of $\delta_r(t)$ and $\dot{\delta}_r(t)$ by taking the *i*th iteration values of $\delta_r(\tau)$ and $\dot{\delta}_r(\tau)$ as the new initial trial conditions.

When the dynamic contact loads are calculated, then the bending and surface contact stresses at the contact points can be obtained by using Eqns (28) and Eqns (33)~(36) respectively.

V. NUMERICAL RESULTS AND DISCUSSION

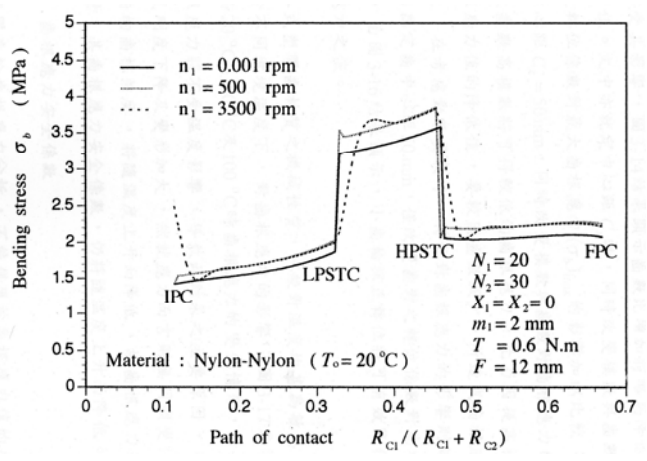

Figure 5: The variation of bending stress along the path of contact.

Nylon gear pair will be used to investigate the effect of temperature on the bending and surface contact stresses. As shown in Fig. 5., the bending stresses are presented at three operating speeds, 0.001, 500, and 3500 rpm . The peak values of bending stresses happen at HPSTC for different operating speeds. W hen the speed increases, the peak value

of bending stresses changes slightly. After 500 rpm , it is found that the peak value keeps approximately a constant.

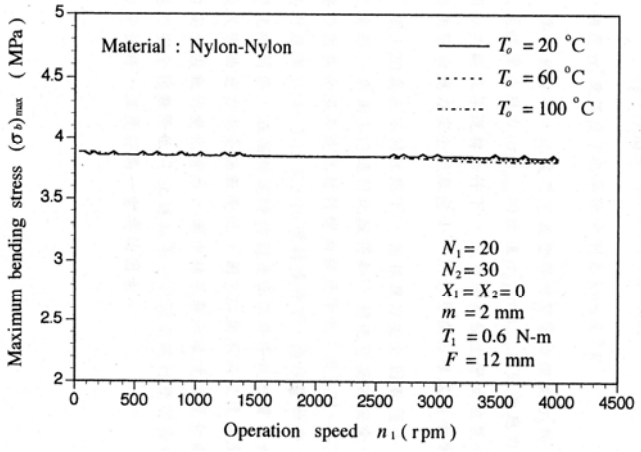

Figure 6: The maximum bending stress at different operating speeds.

For different operating speeds, the m aximum bending stress $(\sigma_b)_{\max}$ does not change very much with regard to the rise of am bient tem perature T_0 , as shown in Fig. 6. However, according to Eqn (31), the bending strength σ_b^* will decrease as the am bient temperature increases. The bending ratio is defined as th e ratio of the bending strength to the m aximum bending stress. As a result, it would be expected that the stress ratio would decrease as the ambient temperature increases. As shown in Fig. 7., it can be found that the bending stress ratio is significantly affected by the ambient temperature. It also can be observed that the operating speed has little influence on the stress ratio if the ambient temperature keeps constant.

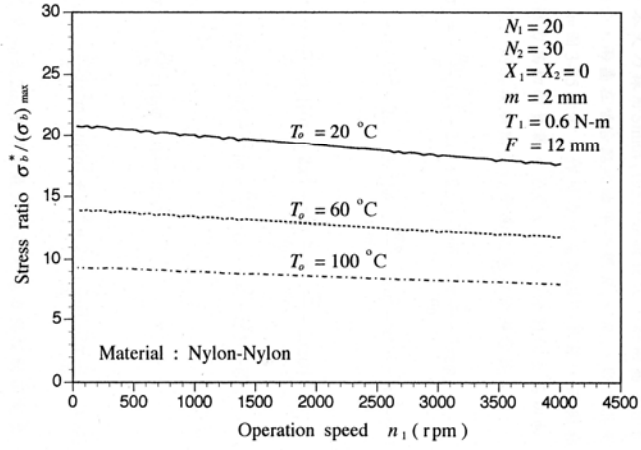

Figure 7: The variation of bending stress along the path of contact.

Similarly, as shown in Fig. 8., the surface contact stresses are presented at thr ee operating speeds, 0.001, 500, and 3500 rpm . The peak values of surface contact stresses happen at HPSTC for 0.001 and 500 rpm. At the speed of 3000 rpm, the peak value of surface contact stresses occurs at the IPC . C ontrary to th e bending stress, the operating speed influences the peak value of surface contact stress a lot.

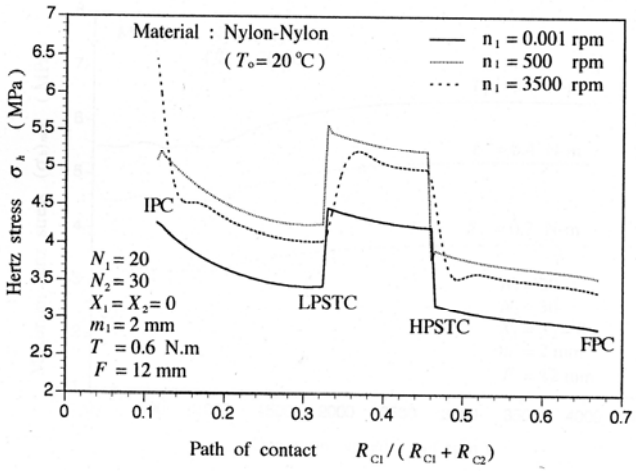

Figure 8: The variation of surface contact stress along the path of contact.

Fig. 9 shows the variati on of m aximum surface contact stress $(\sigma_h)_{\max}$ at different am bient tem peratures. As the ambient tem perature rises, the m aximum surface contact stress lowers. Consulting E qn (41), the surface contact strength σ_h^* decreases too as the am bient temperature increases. Fig. 10 shows the stress ratio at different temperatures. It is observed that high tem perature will weaken the plastic gear with reference to the stress ratio.

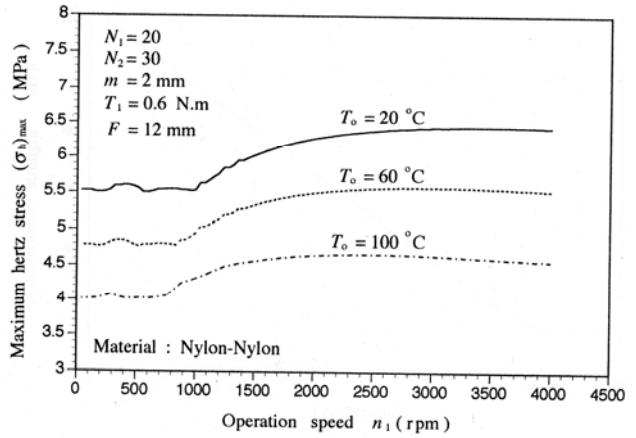

Figure 9: The maximum surface contact stress at different operating speeds.

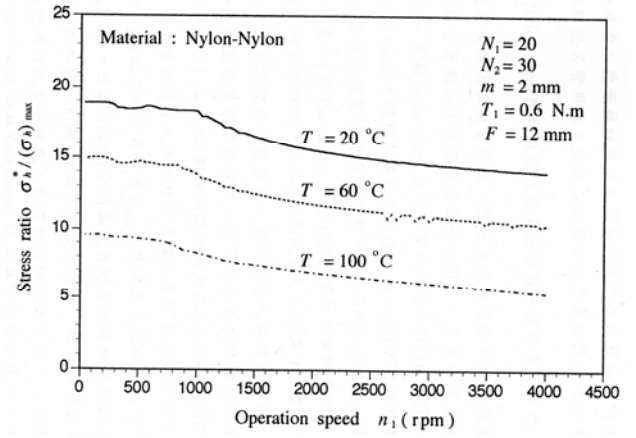

Figure 10: The surface contact stress ratio at different operating speeds.

VI. CONCLUSIONS

In this study, the variation of dynamic fillet bending and surface contact stress distribu tions of the engaging plastic gear pair is discussed. R esults indicate that the stress distributions are quite sensitive to the operating temperature. Generally, the stress peaks are decreased and the stress distributions are spread out in a wider region as the gear bulk temperature is increased. However, since the yield strength is so sensitive to its operating tem perature, a lower safety factor value com es with the high tem perature operation. The fillet bending a nd the surface contact stress peaks are also sensitive to th e engaging speed. A high speed running plastic gear pair alwa ys introduces a higher stress peak and lower safety factor value. Num erical results also show the proposed tem perature dependent dynamic bending stress and surface contact stre sses calculation algorithms are feasible for analyzing the plastic gear pairs.

REFERENCES

[1] Seireg, A., and C onry, T., 1968, "Optimum Design of Gear System s for Surface Durability," *ASME Transactions*, Vol. 11, pp. 321-329.

[2] Gay C. E., 1970, "How to Design to Minimize Wear in Gears," *Machine Design*, Vol. 42, pp. 92-97.

[3] Coy J. J., Townsend D. P., and Zaretsky E. V., 1976, "Dynamic Capacity and Surface Fatigue Life for Spur and Helical Gears," *Trans. of the ASME, Journal of Lubrication Technology*, Vol. 98, No. 2, pp. 267-276.

[4] Moore, W. L., 1979, "Low-Cycle Fatigue and Ultim ate Strength R elated to Gear Design," *Trans of the ASME, Journal of Mechanical Design*, Vol. 101, pp. 373-379.

[5] Savage M ., C oy J. J., and Townsend D. P., 1982, "Optimal Tooth Numbers for C ompact Standard Spur Gear Sets," *Trans of the ASME, Journal of Mechanical Design*, Vol. 104. pp. 749-758.

[6] Carroll R . K., and Johnson G. E., 1984, "Optimal Design of C ompact Spur Gear Sets," *Trans. of the ASME, Journal of Mechanisms, Transmissions, and Automation in Design*, Vol. 106, pp. 95-101.

[7] Lin T. T. C., and Seireg A., 1985, "An Optimum Design Algorithm for Gear System s Incorporating Surface Temperature," *Trans of the ASME, Journal of Mechanisms, Transmissions, and Automation in Design*, Vol. 107, pp. 549-555.

[8] Carroll R. K., and Johnson G. E., 1989, "Dim ensionless Solution to the Optim al Design of Spur Gear Sets," T*rans of the ASME, Journal of Mechanisms, Transmissions, and Automation in Design*, Vol. 111, pp. 290-296.

[9] Errichello R ., 1991, "A R ational Procedure for Designing M inimum-Weight Gears," *Gear Technology*, November/December, pp. 10-14.

[10] Mabie H. H., and Walsh E. J., and B ateman V. I., 1983, "Determination of Hob Offset Required to Generate Nonstandard Spur Gears with Teeth of Equal Strength," *Mechanism and Machine Theory*, Vol. 18, No. 3, pp. 181-192.

[11] Mabie H. H., and Rogers C. A., and R einholtz C. F., 1990, "Design of Spur Gears Generated with Pinion Cutters," *Mechanism and Machine Theory*, Vol. 25, No. 6, pp. 623-634.

[12] Wang K. L., and C heng H. S., 1981, "A Numerical Solution to the Dynam ic Load, Film Thickness and Surface Temperature of Spur Gears: Part I Analysis," *ASME Journal of Mechanical Design*, Vol. 103, pp. 177-187.

[13] Yang D. C. H., and Sun Z. S., 1985, "A Rotary Model for Spur Gear Dy namics," *ASME Journal of Mechanisms, Transmissions, and Automation in Design*, Vol. 107, pp. 529-535.

[14] Arikan M. A. S., and Kaftanoglu B ., 1989, "Dy namic Load and R oot Stress Analy sis of Spur Gears," *Annals of the CRIP* 38, pp. 171-174.

[15] Kuang J. H., and Yu J., 1994, " A Dynamic Model for Addendum M odified Gear Pair," *Proceedings of ASME 1994 Design Technical Conferences,* DE-Vol. 71, pp. 165-176.

[16] Özgüven H. N., and Houser D. R ., 1988, "Mathematical Models Used in Gear Dynam ics - A Review," *Journal of Sound and Vibration*, Vol. 121, pp. 383-411

[17] Tsukamoto, N., 1984, "Investigaton about Load Capacity of Nylon Gears when Tooth Surface Finishing of M ating Steel Gears is different," *Bulletin of JSME*, Vol. 27, No. 229, pp. 1529-1536.

[18] Tsukamoto, N., and Terashim a, K., 1985 "Investigation about the Prevention of Tooth Profile C hange of Plastic Gears," *Bulletin of JSME*, Vol. 28, No. 245, pp. 2723-2729.

[19] Tsukamoto, N., and Maruyama, H., 1991, "A Study on Strength Design M ethods for Plastic Gears," *JSME Int. J.*, Ser. III, Vol. 34, No. 1, pp. 121-126.

[20] Tsukamoto, N., and M aruyama, H., 1993, "B asic Characteristics of Plastic Gears Lubricated with Water," *JSME Int. J.*, Ser. C. Vol. 36, No. 2, pp. 241-250.

[21] Quistwater, J. M . R ., and Dunell, B . A., 1958, "Dynamic M echanical Properties of Ny lon 66 and the Plasticizing Effect of Water Vapor on Ny lon," *J. Polymer Sci.*, Vol. XXVIII, pp. 309-318.

[22] Gang, W., Kohji, T., and M asamichi, K., 1989, "A Study on M echanical Deform ation of Highly Oriented Poly(oxymethylene) by Vibrational Spectroscopy and X-ray Diffraction: Stress and Temperature Dependence of Young's M odulus," *Macromolecules*, Vol. 22, pp. 758-765.

[23] Tsukamoto, N., 1993, "Water Lubrication Characteristics of Polyacetal Gears Filled with Carbon Fibers," *JSME Int. J.*, Serial C, Vol. 36, No. 4, pp. 499-506.

[24] Lancaster, J. K., 1971, "Estim ation of the Limiting PV Relationships for Therm oplastic B earing M aterials," *Tribology*, pp. 82-86.

[25] Kuang J. H., and Yang Y. T., 1992, "An Estim ate of mesh stiffness and Load Sharing R atio of a Spur Gear Pair," *Proceedings of ASME 12th International Power Transmission and Gearing Conference*, Scottsdale, Arizona, DE-Vol. 43-1, pp. 1-10.

[26] Tsukamoto, N., *Bulletin of JSME*, No. 51-469, Ser. C, pp. 2309-2315, 60-9.

[27] Tsukamoto, N., 1992-1, *Bulletin of JSME*, No. 58-545, Ser. C, pp. 231-237.
[28] Smith J. O. and Liu C . K., 1953, “Stresses Due to Tangential and Norm al Loads on Elastic Solid with Application to Som e Contact Problems,” *Journal of Applied Mechanics*, Vol. 20, pp. 157-166.